J|A|C|S COMMUNICATIONS

Published on Web 07/21/2009

A New Photoactive Crystalline Highly Porous Titanium(IV) Dicarboxylate

Meenakshi Dan-Hardi,[†] Christian Serre,*[,†] Théo Frot,[‡] Laurence Rozes,[‡] Guillaume Maurin,[§] Clément Sanchez,*[,‡] and Gérard Férey[†]

Institut Lavoisier, UMR CNRS 8180, Université de Versailles St-Quentin-en-Yvelines, 45 Avenue des Etats-Unis, 78035 Versailles Cedex, France, Laboratoire de Chimie de la Matière Condensée de Paris, UMR CNRS 7574, UPMC- Université Paris VI, Collège de France, 11 place Marcelin Berthelot, 75231 Paris, France, and Institut Charles Gerhardt Montpellier, UMR CNRS 5253, UM2, ENSCM, UM1, Place E. Bataillon, 34095 Montpellier cedex 05, France

Received May 7, 2009; E-mail: serre@chimie.uvsq.fr; clement.sanchez@upmc.fr

Metal organic frameworks (MOFs) are an attractive class of porous solids with potential applications in gas storage, separation, catalysis, thin films, magnetism, or drug delivery.[1−11] Their metallic parts mainly correspond to divalent and trivalent ions of 3d transition metals (Zn, Cu, Fe, Ni, etc.), 3p metals, or lanthanides[3,9,11−14] Among them, titanium is a very attractive candidate due to its low toxicity, redox activity, and photocatalytic properties. So far, incorporation of titanium in porous solids has been restricted to either substitution of silicates in zeolites or the synthesis of titanium phosphates, diphosphonates, or dialcoolates with a limited porosity.[15] In parallel, a large number of titanium oxoclusters based on alkoxydes and carboxylate groups have been described.[16,17] We have initiated a search of highly porous titanium based MOFs using terephthalic acid (BDC or 1,4-benzenedicarboxylic acid) and either inorganic titanium precursors (chloride, sulfates, oxosulfates, nitrates, oxide) or titanium alkoxides under solvothermal conditions (100−200 °C). This led to titanium dioxide or poorly crystalline or dense hybrid phases or a combination of them, as reported by others previously.[18] However, using an appropriate choice of solvent mixtures (dimethylformamide (DMF) and methanol) and titanium tetraisopropoxide at 150 °C, a well crystallized white hybrid solid denoted MIL-125 or $Ti_8O_8(OH)_4$-$(O_2C-C_6H_4-CO_2)_6$, guests have been isolated (MIL stands for Material from Institut Lavoisier). The as-synthesized solid was calcined at 200 °C for extracting the molecules of solvent. Rehydration at 300 K does not change the X-ray powder pattern. The structure was solved *ab initio* on the hydrated solid using X-ray powder diffraction data by a direct method using Expo[19] while the refinement was performed through the Rietveld method with Fullprof and its graphical interface Winplotr (Figure S1, Tables S1−S3).[20,21] Thermal gravimetric analysis and infrared spectroscopy confirm the formula deduced from the structure determination (Figures S2, S3).

The quasi-cubic tetragonal structure can be easily described as an augmented version[22] of the centered cubic structure (Figure 1a) in which the atoms are substituted by cyclic octamers (SBU-8) of edge- and corner-sharing $TiO_5(OH)$ octahedra (Figure 1b). 1,4-Benzene dicarboxylates (BDC) replace the contacts between atoms, link the octamers, and provide a 3D structure (Figure 1c). As in a *cc* packing, each octamer has 12 SBU neighbors, connected by the BDC ligands. Four linkers are in the plane of the octameric wheel, four are above and four below. The 3D arrangement provides two types of cages corresponding to the octahedral (Figure 1d) and tetrahedral (Figure 1e) vacancies of a *cc* packing. Their effective

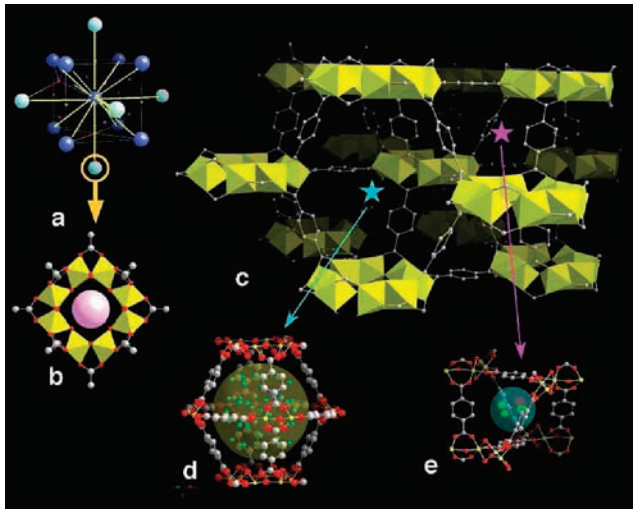

Figure 1. (a) Perspective view of a centered cubic (*cc*) arrangement; the 12-fold coordination is evidenced by yellow lines. Purple and orange dots indicate the positions of the centers of the tetrahedral and octahedral vacancies. (b) View of the perforated cyclic octamer with edge- and corner-sharing Ti octahedra; it corresponds to the atom with an orange circle of the classical *cc* packing through the SBU augmentation. (c) Perspective view of MIL-125 with the central octamer surrounded by 12 others; the pink and blue stars indicate the centers of the tetrahedral and octahedral vacancies in MIL-125. (d) Ball and stick representation of the octahedral vacancy, filled by water molecules (in green); the large yellow sphere represents the effective accessible volume of the cage. (e) The tetrahedral vacancy; in (d) and (e) the color code is as follows: carbon, gray; oxygen, red; water, green; titanium, yellow.

accessible diameters are 12.55 and 6.13 Å, taking into account the van der Waals radius of carbons (1.7 Å), which are closer to the center of each cage. The triangular windows of the cages are responsible for the strong rigidity of the structure.[23] They exhibit free apertures in the range 5−7 Å and provide easy access to the different cages as seen in Figure 1d and 1e, which evidence also the water molecules trapped in the two cages. Oxo and hydroxo groups are present at the core of the SBU. Unfortunately, due to the use of powder data, it is not possible to clearly discriminate oxygen atoms from oxo and hydroxo moieties, while IR spectroscopy confirms the presence of μ_2(OH) hydroxo groups (see shoulder at 3700 cm^{-1} in Figure S2).

It is worth noting that the only MOFs with 12 connected SBUs are still scarce.[24] Octameric SBUs of metal octahedral have never been encountered in three-dimensional MOFs before. It was however found previously in a molecular chromium(III) hydroxoacetate.[25] Only hydroxo groups are present at the core of the SBU due to the difference in charge between chromium(III) and

[†] Université de Versailles St-Quentin-en-Yvelines.
[‡] Université Paris VI.
[§] ENSCM.

titanium(IV) (Figure S4). MIL-125 can therefore be considered as a 3D reticulated analogue of the chromium acetate molecular structure. Comparison of the Cr hydroxyacetate (Figure S5) and MIL-125 evidences interesting similarities. Both structures are tetragonal with a I lattice. In both, the octamers are stacked along [001], but the manner of packing differs in the two structures. MIL-125 is constrained by the linkage of the dicarboxylates, whereas the molecular character of the hydroxyacetate gives some freedom for the arrangement of the octamers. The structure of the hydroxyacetate can also be considered as the interpenetration of two I lattices (translation vector 0; $^1/_2$; $^1/_4$), each of them corresponding to the arrangement encountered in MIL-125 (Figure S5). One could thus imagine that exchange of acetates by terephthalates induces the constrained movement (Figure S6) of the free octamers to realize, through the connection of the linkers, the framework of MIL-125.

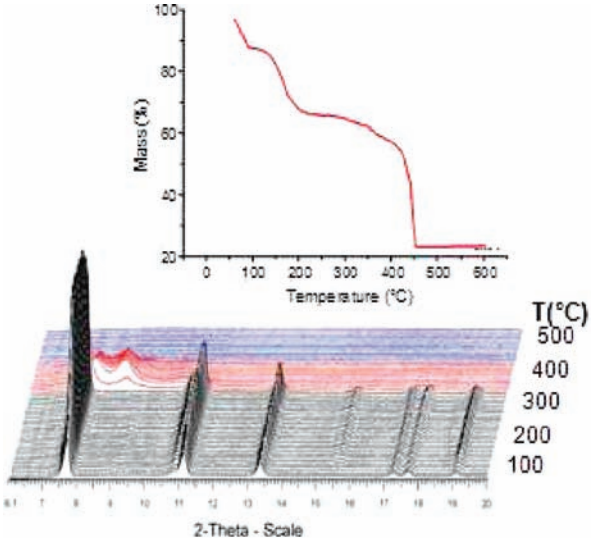

Figure 2. X-ray thermodiffractometry ($\lambda_{Co} \approx 1.79$ Å) under air of MIL-125. Each color represents a different phase. The thermal gravimetric analysis of MIL-125 (under air) is represented as an insert at the top of the figure.

MIL-125 is thermally robust. During the departure of the guest molecules below 200 °C followed by thermal gravimetric analysis, X-ray thermodiffractometry (Figure 2) does not indicate any change in crystallinity. A phase transition occurs between 290 and 350 °C, characterized by a strong change in peak positions and a decrease in crystallinity, before the collapse of the solid above 360 °C. This structural reorganization at ca. 300 °C is probably related to the departure of hydroxo groups, evidenced by the small weight loss of 4−5% at this temperature range. Further studies are however needed to analyze in detail this phase transition.

Nitrogen sorption experiments reveal that MIL-125 is highly porous with a type I isotherm characteristic of microporous solids, a BET surface area of 1550(20) $m^2 \cdot g^{-1}$, and a micropore volume of 0.65(2) $cm^3 \cdot g^{-1}$ (Figure S7). We have also estimated, using an appropriate Monte Carlo algorithm, the accessible theoretical BET surface area, for a nitrogen sized probe molecule, of MIL-125 to be close to 2140 $m^2 \cdot g^{-1}$ (Figure S8 and details in the Supporting Information (SI)).[26] Indeed, chemical analyses show an excess of both C and Ti compared to the theoretical values (see SI). As evidenced by the band at 1710 cm^{-1} in the IR spectrum (Figure S3), the excess of C comes from the existence of free H_2BDC within the pores (corresponding to 0.3 BDC/unit cell), inducing a partial blocking of the pores. The excess of Ti could be explained by the formation of amorphous TiO_2 (0.75 TiO_2/u.c.) during the synthesis.

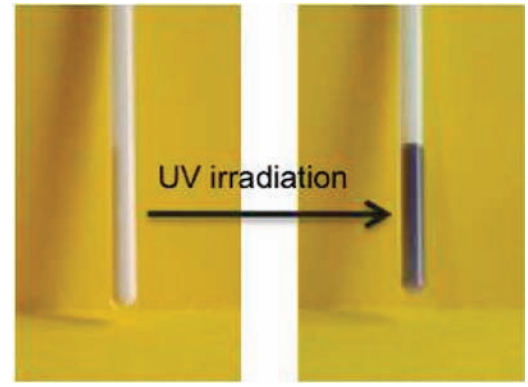

Figure 3. View of MIL-125 in a capillary filled with benzyl alcohol before and after UV irradiation.

The high surface area of MIL-125 allows a large adsorption of organic molecules. In particular, when alcohols (R−OH) such as methanol, ethanol, and benzylalcohols are adsorbed inside the MIL-125 framework under nitrogen, a fast photochromic effect is observed upon UV−visible excitation. The light irradiation changes the color of the materials from white to purple-gray-blue within a few seconds. After a few minutes, an intense gray-blue color is observed (Figure 3). The characteristic photoinduced absorption spectrum of MIL-125 is shown in Figure S9. With the colored photochromic sample of MIL-125, the light absorption spectrum exhibits new broad and intense bands in the visible−near-IR range (400−800 nm) with two maxima located at 500 and 596 nm. These electronic transitions are close to those reported for photoreduced hybrid nanocomposites made of titanium-oxo aggregates and PHEMA polymers[27] and can be assigned to d−d transitions and to intervalence transitions respectively. This photochromic behavior can be associated with the presence of the intervalence electron transfer bands resulting from the optically induced hopping of electrons from Ti(III) to Ti(IV) sites in the titanium oxo-clusters of MIL-125. To determine if this phenomenon is due to the presence of residual amorphous TiO_2, the same experiment was conducted using a commercial P25 TiO_2 sample and compared the one performed with MIL-125 (Figure S10). Clearly, a very strong dark blue coloration was observed with the MOF in contrast with a weak blue coloration of the oxide sample. This is in agreement with a longer lifetime of the reduced state within MIL-125 and thus a much higher efficiency of the photoactivation. Such behavior was also observed previously with titanium oxo-PHEMA nanocomposites upon strong laser-induced activitation.[27b]

The presence of Ti(III) species was confirmed by ESR spectroscopy carried out with the colored MIL-125. After alcohol adsorption, the EPR spectra recorded at 75 K for UV-irradiated MIL-125 is shown in Figure S9. It exhibits the characteristic parameters of paramagnetic Ti^{3+} centers in a distorted rhombic oxygen ligand field ($g_x = 1.970$, $g_y = 1.938$, and $g_z = 1.900$).[28] An ESR line broadening is observed at room temperature (Figure S11), due to hopping of the unpaired electron between Ti(III) and Ti(IV) ions likely thermally activated through the vibrations of the titanium-oxo clusters,[29] which is characteristic from the mixed-valence properties of partially reduced titanium-oxo clusters. Moreover, the reversibility of the coloration is demonstrated by the coloration fading of the dark sample in the presence of air. However, DMF washed and dried MIL-125 do not change their color upon UV irradiation. Correspondingly, the ESR spectrum at 75 K of the light irradiated dry MIL-125 does not exhibit the characteristic feature of Ti(III) species. Therefore, this photoassisted reduction of Ti(IV) into Ti(III) is coupled with the oxidation of

the alcoholic functions of alcohols, as demonstrated by the presence of aldehydes by IR spectroscopy (Figure S12), as usually observed for photooxidizing processes.[30] This photochemical oxidation of alcohols is of interest because it underlines a possible photocatalytic activity for titanium-oxoclusters based MOFs such as MIL-125. Indeed, the ESR spectrum (Figure S13, 75 K) of irradiated MIL-125 (left in air) exhibits an anisotropic weak signal centered around $g = 2$. A careful analysis of its shape yields the following fitted values: $g_x = 2.02$, $g_y = 2.01$, $g_z = 2.00$. The observed resonances are similar to the characteristic orthorhombic signals reported for super oxide diatomic $[O_2]^-$ ions adsorbed on metal oxide surfaces. In addition, the g values are close to those already reported for $[O_2]^-$ adsorbed at the surface of titania ($g_x = 2.025$, $g_y = 2.009$, $g_z = 2.003$; $g_x = 2.03$, $g_y = 2.008$, $g_z = 2.004$).[31,32] The largest measured g value ($g = 2.02$) is in good agreement with prediction of the ionic model for a cation of charge 4 (titanium(IV)) as an adsorption surface site. This back photo-oxidation of titanium(III) ions into titanium(IV) can be associated with the reduction of molecular oxygen into superoxide diatomic $[O_2]^-$ ions, with no destruction of the framework (Figure S14). The photoinduced paramagnetic signals can be correlated with the photocatalytic effect promoted by MIL-125, yielding to the photo-oxidation of alcohols. For the initial steps, taking into account the transfer of one electron and one proton, the following hypothetical scheme is proposed (Figure 4), with probable superoxide diatomic O_2^- ions, in the presence of protons yielding hydrogen peroxide.

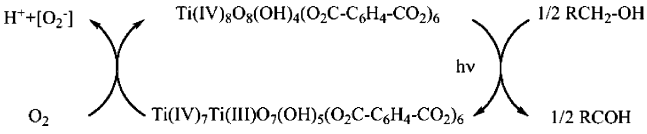

Figure 4. Proposed mechanism of reduction of MIL-125 in the presence of alcohols under UV radiation.

In conclusion, we report the synthesis and structure of a new highly porous MOF constructed from titanium-oxo-hydroxo clusters and dicarboxylate linkers. Moreover, a reversible photochromic behavior induced by alcohol adsorption is observed. The resulting hybrid material exhibits high photonic sensitivity, inherent to the titanium-oxo component. UV−visible irradiation promotes the formation of a Ti(III)−Ti(IV) mixed valence MIL-125. This confinement of photoinduced electrons as titanium(III) centers inside the titanium-oxo-hydroxo clusters assures, under nitrogen, efficient trapping and long-term stability of the photoinduced mixed valence compound therefore providing stable coloration. The reduction of titanium centers and oxidation of adsorbed alcohol molecules occur simultaneously. In the presence of oxygen, the titanium oxocluster is back oxidized, emphasizing a possible photocatalytic property of titanium-oxo based MOFs. Moreover, the easy reduction of metallic titanium centers to produce mixed valence compounds offers ample scope for new microporous hybrid solids capable of fitting applications in different fields as smart photonic devices, sensors, and catalysis.

Acknowledgment. Authors gratefully acknowledge the financial support of the European Commission though the FP6 STREP program "DeSANNS" (SES6-CT-2005-020133).

Supporting Information Available: Full ref 14. Crystallographical details. Experimental conditions. TGA, IR, BET. Details of the photochromism (EPR, ESR, UV, etc.). Surface area calculations. This material is available free of charge via the Internet at http://pubs.acs.org.

References

(1) Férey, G. *Chem. Soc. Rev.* **2008**, *37*, 191–214.
(2) Mueller, U.; Schubert, M.; Teich, F.; Puetter, H.; Schierle-Arndt, K.; Pastre, J. *J. Mat. Chem.* **2006**, *16*, 626–636.
(3) Kitagawa, S.; Kitaura, R.; Noro, S.-I. *Angew. Chem., Int. Ed* **2004**, *43*, 2334–2375.
(4) (a) Wong-Foy, A. G.; Matzger, A. J.; Yaghi, O. M. *J. Am. Chem. Soc.* **2006**, *128*, 3494. (b) Kaye, S. S.; Long, J. R. *J. Am. Chem. Soc.* **2006**, *127*, 6506. (c) Mulfort, K. L.; Hupp, J. T. *Inorg. Chem.* **2008**, *47* (18), 7936–7938.
(5) (a) Serre, C.; Bourrelly, S.; Vimont, A.; Ramsahye, N. A.; Maurin, G.; Llewellyn, P. L.; Daturi, M.; Filinchuk, Y.; Leynaud, O.; Barnes, P.; Férey, G. *Adv. Mater.* **2007**, *19*, 2246–2251. (b) Matsuda, R.; Kitaura, R.; Kitagawa, S.; Kubota, Y.; Belosludov, R. V.; Kobayashi, T. C.; Sakamoto, H.; Chiba, T.; Takata, M.; Kawazoe, Y.; Mita, Y. *Nature* **2005**, *436*, 238–241.
(6) (a) Bastin, L.; Barcia, P. S.; Hurtado, E.J.; C.; Silva, J. A.; Rodrigues, A. E.; Chen, B. *J. Phys. Chem. C* **2008**, *112*, 1575. (b) Alaerts, L.; Kirshhock, C. E. A.; Maes, M.; van der Veen, M. A.; Finsy, V.; Depla, A.; Martens, J. A.; Baron, G. V.; Jacobs, P. A.; Denayer, J. F. M.; De Vos, D. E. *Angew. Chem., Int. Ed.* **2007**, *46*, 4293–4297.
(7) Seo, J. S.; Whang, D.; Lee, H.; Jun, S. I.; Oh, J.; Jeon, Y. J.; Kim, K. *Nature* **2000**, *404*, 982–986.
(8) Scherb, C.; Biemmi, E.; Bein, T. *Angew. Chem., Int. Ed.* **2008**, *47*, 5777–5779.
(9) Guillou, N.; Livage, C.; Drillon, M.; Férey, G. *Angew. Chem., Int. Ed* **2003**, *115*, 5472.
(10) (a) Horcajada, P.; Serre, C.; Vallet-Regí, M.; Sebban, M.; Taulelle, F.; Férey, G. *Angew. Chem., Int. Ed.* **2006**, *45*, 5974–5978. (b) Horcajada, P.; Serre, C.; Maurin, G.; Ramsahye, N. A.; Balas, F.; Vallet-Regí, M.; Sebban, M.; Taulelle, F.; Férey, G. *J. Am. Chem. Soc.* **2008**, *130*, 6774–6780.
(11) Kim, J.; Chen, B.; Reineke, T. M.; Li, H.; Eddaoudi, M.; Moler, D. B.; O'Keeffe, M.; Yaghi, O. M. *J. Am. Chem. Soc.* **2001**, *123*, 8239.
(12) Serre, C.; Millange, F.; Surblé, S.; Férey, G. *Angew. Chem., Int. Ed.* **2004**, *43*, 6286–6289.
(13) Volkringer, C.; Popov, D.; Loiseau, T.; Guillou, N.; Férey, G.; Haouas, M.; Taulelle, F.; Mellot-Draznieks, C.; Burghammer, M.; Riekel, C. *Nat. Mater.* **2007**, 760–764.
(14) Park, Y.; Ket al, *Angew. Chem., Int. Ed.* **2007**, *46*, 8230–8233.
(15) (a) Serre, C.; Taulelle, F.; Férey, G. *Chem. Commun.* **2003**, 2755–2765 (Feature Article). (b) Serre, C.; Groves, J. A.; Lightfoot, P.; Slawin, A. M. Z.; Wright, P. A.; Stock, N.; Bein, T.; Haouas, M.; Taulelle, F.; Férey, G. *Chem. Mater.* **2006**, *18*, 1451–1457. (c) Chuck, C. J.; Davidson, M. G.; Jones, M. D.; Ko1hn, G. C.; Lunn, M. D.; Wu, S. *Inorg. Chem.* **2006**, *45*, 6595–6597.
(16) Rozes, L.; Steunou, N.; Fornasieri, G.; Sanchez, C. *Monatsh. Chem.* **2006**, *37*, 501–528.
(17) (a) Schubert, U. *Chem. Mater.* **2001**, *13*, 3487–3494. (b) Schubert, U. *J. Mater. Chem.* **2005**, *15*, 3701–3715.
(18) Sabo, M.; Böhlmann, W.; Kaskel, S. *J. Mater. Chem.* **2006**, *16*, 2354.
(19) Altomare, A.; Burla, M. C.; Camalli, M.; Carrozzini, B.; Cascarano, G. L.; Giacovazzo, C.; Guagliardi, A.; Moliterni, A. G. G.; Polidori, G.; Rizzi, R. *J. Appl. Crystallogr.* **1999**, *32*, 339.
(20) Rodriguez-Carvajal, J. *Collected Abstracts of Powder Diffraction Meeting*; Toulouse, France, 1990; p *127*.
(21) Roisnel, T.; Rodriguez-Carvajal, J. *Abstracts of the 7th European Powder Diffraction Conference*; Barcelona, Spain, 2000; p *71*.
(22) O'Keeffe, M. *Z. Kristallogr.* **1991**, *196*, 21–37.
(23) Férey, G.; Serre, C. *Chem. Soc. Rev.* **2009**, *38*, 1380.
(24) (a) Cavka, J. H.; Jakobsen, S.; Olsbye, U.; Guillou, N.; Lamberti, C.; Bordiga, S.; Lillerud, K. P. *J. Am. Chem. Soc.* **2008**, *130*, 13850–1385. (b) Zhang, X.-M.; Fang, R.-Q.; Wu, H.-S. *J. Am. Chem. Soc.* **2005**, *127*, 7670. (c) Li, D.; Wu, T.; Zhou, X. P.; Zhou, R.; Huang, X. C. *Angew. Chem., Int. Ed.* **2005**, *44*, 4175.
(25) Eshel, M.; Bino, A.; Felner, I.; Johnston, D. C.; Luban, M.; Miller, L. L. *Inorg. Chem.* **2000**, *39*, 1376–1380.
(26) Düren, T.; Millange, F.; Férey, G.; Walton, K. S.; Snurr, R. Q. *J. Phys. Chem. C* **2007**, *111*, 15350–15356.
(27) (a) Kuznetsov, A. I.; Kameneva, O.; Bityurin, N.; Rozes, L.; Sanchez, C.; Kanaev, A. *Phys. Chem. Chem. Phys.* **2009**, *11*, 1248–1257. (b) Kameneva, O.; Kuznestov, A. I.; Smirnova, L. A.; Rozes, L.; Sanchez, C.; Alexandrov, A.; Bityurin, N.; Chhor, K.; Kanaev, A. *J. Mater. Chem.* **2005**, *15*, 3380–3383.
(28) Goodman, B. A.; Raynor, J. B. *Adv. Inorg. Chem. Radiochem.* **1970**, *13*, 185.
(29) Robin, M. B.; Day, P. *Adv. Inorg. Chem. Radiochem.* **1967**, *10*, 247.
(30) Hill, C. L.; Bouchard, D. A. *J. Am. Chem. Soc.* **1985**, *107*, 5148–5157.
(31) Cordoncillo, E.; Guaita, F. J.; Escribano, P.; Philippe, C.; Viana, B.; Sanchez, C. *Opt. Mater.* **2001**, *18*, 309.
(32) Naccache, C.; Meriaudeau, P.; Che, P.; Trench, A. J. *Trans. Faraday Soc.* **1971**, *67*, 506–512.

JA903726M